RESEARCH REPORT 125

A SHOCK TUBE STUDY OF THE COUPLING OF THE O_2 - Ar RATES OF DISSOCIATION AND VIBRATIONAL RELAXATION

by

Kurt L. Wray

AVCO-EVERETT RESEARCH LABORATORY
a division of
AVCO CORPORATION
Everett, Massachusetts

Contract No. DA-19-020-ORD-5476

January 1962

prepared for

ADVANCED RESEARCH PROJECTS AGENCY
monitored by the
ARMY ROCKET AND GUIDED MISSILE AGENCY
ARMY ORDNANCE MISSILE COMMAND
UNITED STATES ARMY
Huntsville, Alabama

ABSTRACT

At low temperatures the vibrational relaxation time, τ_v, is much shorter than the dissociation time, τ_d. The O_2 - Ar results of Camac (J. Chem. Phys. 34 448 (1961)) and Camac and Vaughan (Ibid, p. 460) yield a $\tau_d/\tau_v = 60$ at 5000°K and, upon extrapolation, a $\tau_d/\tau_v = 1.4$ at 18000°. According to these extrapolations, dissociation at high temperatures would proceed significantly before vibrational equilibration would occur. The purpose of this investigation was to determine how the dissociation rate will be affected by a lack of vibrational equilibrium.

Studies of the dissociation rate of dilute O_2 - Ar mixtures were made in a 24" diameter shock tube from 5000 - 18000°K. The O_2 concentration was monitored by its absorption of 1470A radiation. An Arrhenius plot of the data yielded a straight line from 5000 - 11000°K, the rate constant being given by $k_d = 2.9\ (\pm\ 12\%) \times 10^{14} \exp(-D/RT)$ cc/mole-sec. Above 11000° the data deviate from the line given by this equation - at 18000° k_d being .45 times the calculated value.

An incubation time, Δt, was observed during which dissociation does not proceed to a significant extent. The ratio of this incubation time to the vibrational relaxation time (obtained by extrapolating Camac's low temperature results) when plotted against translational temperature, displays a slight negative temperature dependence. At 18000° $\Delta t/\tau_v = 0.4$, at 8000° $\Delta t/\tau_v = 1$, and at 5500° we estimate that $\Delta t/\tau_v \approx 2$.

I. Introduction

The rates of dissociation and vibrational relaxation of oxygen for the catalytic species Ar, O_2 and O are now reasonably well determined up to T = 7500°K. We quote here for the rate of dissociation of oxygen by argon the results of Camac and Vaughan[1]

$$k_d = 3.6 \times 10^{18} \quad T^{-1} \exp(-D/RT) \quad \text{cc/mole-sec} \quad , \tag{1}$$

where D = 118000 cal/mole. A dissociation relaxation time, τ_d, is defined by

$$1/\tau_d = k_d \left(n_{Ar}/N_0 \right) \quad , \tag{2}$$

where n_{Ar} is the number of argon atoms/cc and N_0 is Avogadro's number.

For the vibrational relaxation time, τ_v, of O_2 by Ar, Camac[2] gives

$$1/\tau_v = 1.2 \times 10^{-7} \quad T^{1/6} \left[1-\exp(-2228/T) \right] \exp(-1.04 \times 10^{7}/T)^{1/3} n_{Ar} \text{ sec}^{-1}. \tag{3}$$

These equations are plotted in Fig. 1 setting $n_{Ar} = 1.28 \times 10^{17}$.*

At low temperatures the vibrational relaxation process is much faster than the dissociation process. Hence, the rate constant which is determined for the latter process is for a gas essentially in vibrational equilibrium. As the temperature is increased the rates of both processes increase but the dissociation rate increases faster; according to Fig. 1, at T = 5000°K, $\tau_d/\tau_v = 60$; at T = 8000°, $\tau_d/\tau_v = 5.4$ and at T = 18000°, $\tau_d/\tau_v = 1.4$. These ratios are independent of density. Hence, at temperatures above about 8000°, on the basis of the above extrapolations, one would expect that dissociation would proceed to a significant extent before

* This particle density corresponds to T = 300°K and P = 4mm (or an initial shock tube pressure of P_1 = 1mm and a density ratio across the shock of $\rho_2/\rho_1 = 4$). This density was chosen as it corresponds to the experimental conditions used in this study.

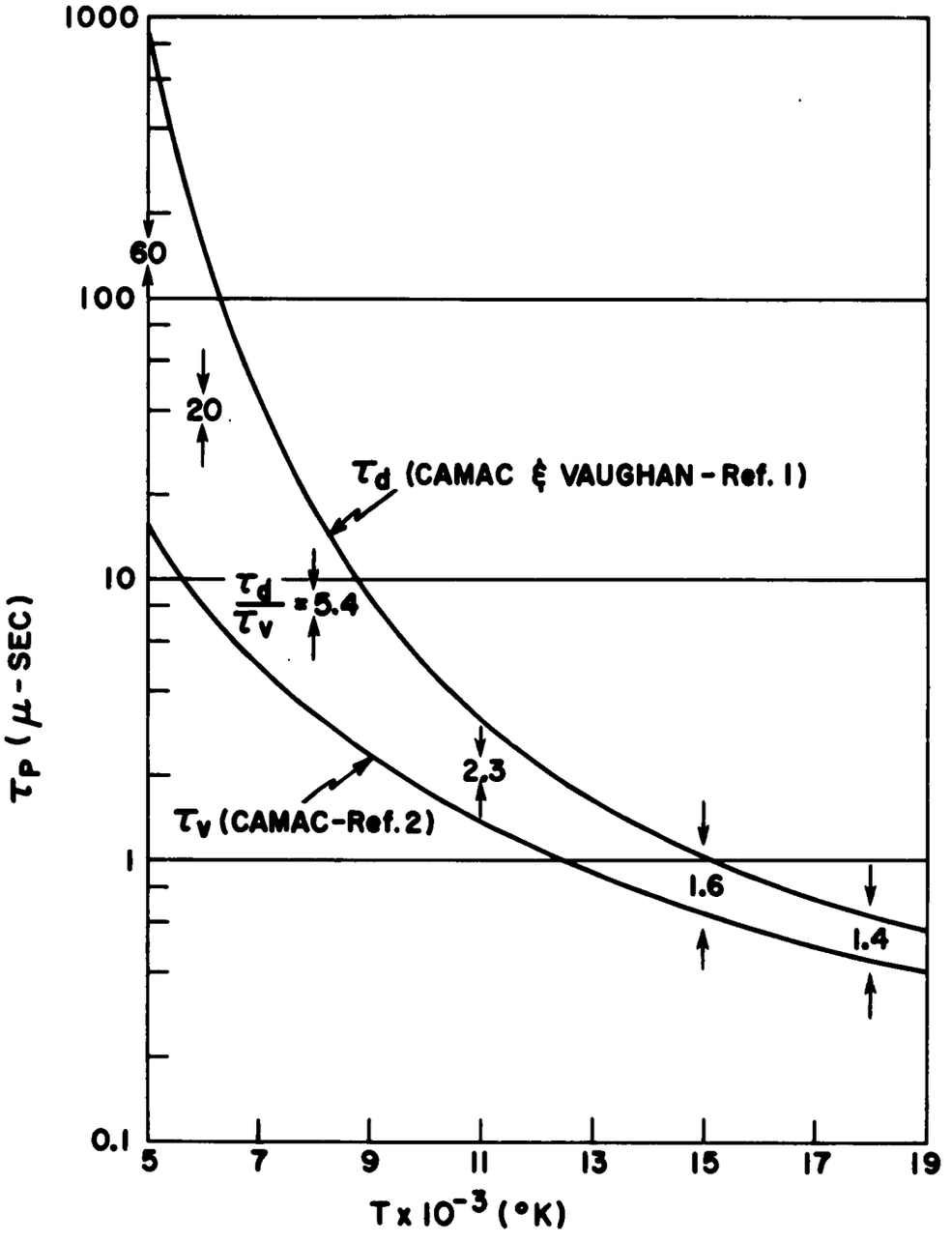

Fig. 1 The dissociation and vibrational relaxation times in the particle coordinate system at a density of $n_{Ar} = 1.28 \times 10^{17}$ particles/cc plotted as a function of temperature. The τ_d is extrapolated from experimental results above 7500°, τ_v above 7000°. Also indicated in the figure is the density independent ratio τ_d/τ_v at several temperatures.

7441

vibrational equilibrium obtains. The purpose of this experimental study was to determine how the dissociation rate will be affected by this situation, i.e., to what extent the dissociation and vibrational processes couple.

Camac did his work in a 1.5 inch diameter shock tube where it was not possible to obtain adequate resolution at temperatures at which coupling of vibration and dissociation might become important. However, by using a 21.5% O_2 - 78.5% Ar mixture at an initial pressure of 0.93mm he did observe a coupling effect at temperatures around 9000°. It should be noted that with such a rich O_2 mixture, there are large temperature changes behind the shock front as the O_2 relaxes; this tends to complicate the data analysis. Camac states that his data show that dissociation "is in progress during the vibrational relaxation" although it is slower "by more than a factor of 2".

In the present work, the dissociation of dilute O_2-Ar mixtures has been measured using a 24" diameter shock tube available at this laboratory.[3] This facility allows the production of shock waves at the low initial densities necessary to slow down the relaxation processes sufficiently to be well resolved. Furthermore, the long optical path allows a low partial pressure of O_2, hence, essentially isothermal and isobaric conditions behind the shock. The temperature range covered in this investigation was 5000 - 18000°K. The O_2 concentration was monitored as a function of time behind the incident shock wave by its absorption of 1470A radiation - similar to the work of Camac.

Camac[2] has measured the absorption coefficient of oxygen at 1470A as a function of its vibrational temperature and showed that this absorption coefficient is independent of the rotational and translational temperature of the gas. At room temperature the absorption coefficient per cm of path length at a density corresponding to 300° and one atmosphere pressure is 315. He found that this coefficient decreases monotonically as the vibrational temperature is increased, and asymptotically approaches the value of 135 at about 7500° and remains constant thereafter. Although his measurements of this absorption coefficient

were carried just a little past 8000°, theoretical arguments justify assuming that it remains constant as one continues to increase the temperature. These results are plotted in Fig. 2.

At the high end of the temperature range covered in the present work the equilibrium ionization of the argon diluent is very significant and the energy invested in ionization would cause the temperature to drop many thousands of degrees. In order to ascertain whether or not ionization did occur during the vibrational and chemical relaxation of the small amount of O_2 in the gas, the electron density was monitored using a microwave technique.[4]

II. The Apparatus

The shock tube used in this work was designed and built by Lin[3] for his investigations of the ionization rate in shock-heated air, although for the present work a new test section was built. The tube is of stainless steel construction having a length of 60' and a diameter of 2'. The driver section is 6' long and the diaphragm is ruptured by igniting H_2-O_2-N_2 mixtures at high pressure. Shock speeds were determined using painted platinum strip heat transfer gages.

Because there was some concern over the possibility of the shock wave being tilted with respect to the shock tube walls, four heat transfer gages were mounted around the circumference of the shock tube 90° apart just in front of the optical station. The signals from two of these gages were delayed three microseconds and put into the -B channels of the differential amplifiers of a dual beam scope. The two undelayed signals were put into the +A channels. In this way we could correlate the time of arrival of the shock wave at the four heat transfer gages. Under no conditions in these studies was the shock front tilt found to be significant (i.e., it was less than the optical slit width).

At low densities a shock front in a shock tube is curved to a significant extent. Lin[3] has measured the shock front curvature as a

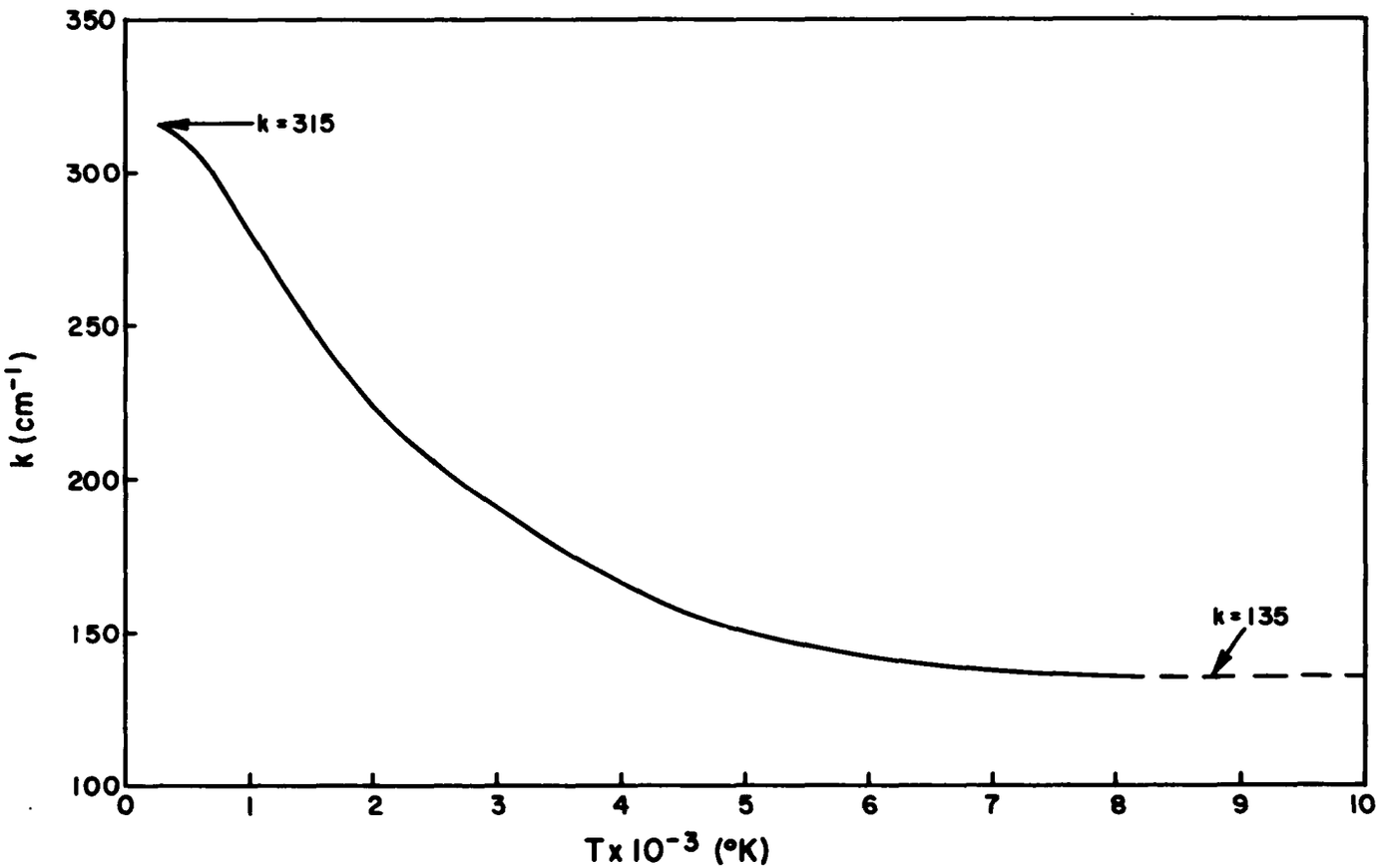

Fig. 2 The oxygen absorption coefficient at 1470A per cm of path length at a density corresponding to 300°K and one atmosphere pressure. These data were taken from Ref. 2.

function of initial pressure and shock speed for air shocks in this 24" diameter tube. He found the shock front curvature (defined as the distance along the center line from the shock front to the plane formed by the intersection of the shock front and the shock tube walls) to be independent of the shock speed and to vary inversely as the square root of the initial pressure. His data for curvature, δ, as a function of initial pressure P_1, can be fit by the following equation:

$$\delta \text{ (mm)} = 1.75\ P_1^{-1/2} \text{ (mm of Hg)} \quad . \qquad (4)$$

At the lowest initial pressures used in these experiments (1/4 mm), the shock front curvature would amount to 3.5 mm. The optical slits used for all the experiments were 1 mm wide, hence, a shock front curvature of 3.5 mm represents a serious loss in resolution. To avoid this difficulty the optical path was reduced to 12" by inserting 1" diameter, 6" long pipes into opposite sides of the shock tube. (See Fig. 3.) Each of these pipes was terminated inside the shock tube by a flat plate 2.5" high and 1.5" wide, the edges of which were tapered at an angle of 9° 44' to form knife edges. * The center of each knife-edged plate contained a flush calcium fluoride window 1/2" in diameter and 3/8" thick; behind each window, i.e., inside the pipe was located the 1/2" high, 1mm wide slit. Assuming the shock front surface to be spherical, the amount of curvature between two parallel planes placed within the shock tube decreases as the square of the ratio of the distance between the two planes to the shock tube diameter. Hence, for the 1/4 mm runs the shock front curvature was effectively reduced to .87 mm. Furthermore, this technique reduces the problem of 0-atom recombination in the cold, dense boundary layer since on

* The width of the plate was arrived at by making the leading edge project twice the standoff distance of the bow shock formed in front of the pipe and the height was such that the Mach wave formed at the upper and lower corners of the leading edge would not cross the window located at the center of the plate.

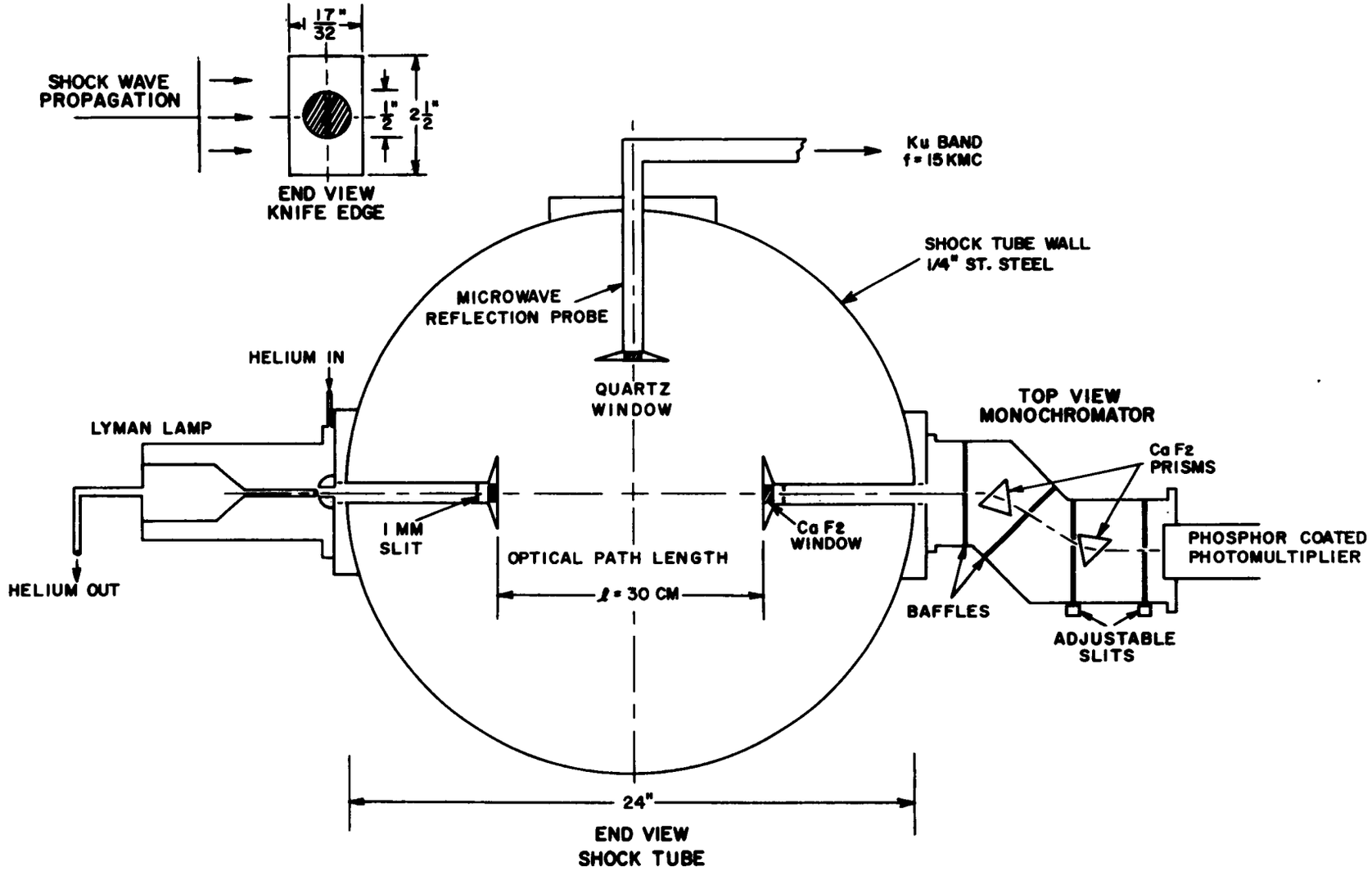

Fig. 3 Schematic diagram of the shock tube test section. Both the U. V. optical system and the microwave system are shown.

these plates the boundary layer grows only to a steady state thickness instead of growing continuously as on the shock tube wall.

The light source was located externally to the shock tube at the entrance to one of these pipes (see Fig. 3). The light source was a Lyman lamp, which produced an oscillating output whose second cycle maximum was flat for about 20 microseconds (see Ref. 2 for a description of this light source). This lamp was triggered from one of the upstream heat transfer gages through a time-delay generator which was pre-set to synchronize the second cycle light maximum with that of the shock wave arrival at the optical station. The monochromator, consisting of two calcium fluoride prisms and necessary light baffles, was located outside the shock tube at the entrance to the other pipe. A photomultiplier coated with sodium salicylate phosphor was mounted within the monochromator just behind the exit slit. In use, the monochromator was evacuated. The output of the photomultiplier was monitored on an oscilloscope. This oscilloscope was triggered by a heat transfer gage located about one inch in front of the optical station.

The electron density monitor was mounted perpendicular to the U. V. system. In this case the wave guide itself served as the six inch pipe extending into the shock tube. It was also terminated by a knife-edged plate similar to that of the U. V. system, the open end of the wave guide being covered by an oblong quartz window (height = .311", width = .622"). The microwave frequency used was $f = 1.5 \times 10^{10}$ cps (Ku band). Before each run, the maximum deflection of the oscilloscope trace from the reflected microwave signal was set by shorting out the wave guide (corresponding to complete reflection). This microwave reflection signal was displayed on a dual beam scope, the other beam of which displayed the U. V. signal.

III. Data Reduction

Three different composition O_2-Ar mixtures were used, they were: 4% O_2 (P_1 ~1/4 mm), 2% O_2 (P_1 ~1 and 1/2 mm) and 1/2% O_2 (P_1 ~4 and 10 mm). The richer mixtures were employed at higher

temperatures where lower densities were necessary to allow resolution. At lower temperatures, where the rate processes are slower, higher densities could be used in conjunction with smaller O_2 partial pressures. This is a desirable situation since the relaxation processes are most temperature dependent at low temperatures.

For each of the three different mixtures studied, shock tube performance data were computed and plotted. We show here only the curves for the 4% O_2 - 96% Ar mixture. Figure 4a shows the temperature behind the shock, T_2, and Fig. 4b gives the density ratio across the shock, ρ_2/ρ_1, both plotted as functions of the shock speed, U_s. The three curves on each graph give the conditions when equilibration of the shocked gas has proceeded to the states: i) translational and rotational equilibrium only, ii) translational, rotational, electronic and vibrational equilibrium only, and iii) full equilibrium - but without ionization. In Fig. 4b, the increase of ρ_2/ρ_1 at large U_s for the "Full Eq" curve is due to electronic excitation of the atoms. The "Vib Eq" curve actually crosses the "Full Eq" curve due to the fact that more energy is invested in electronic excitation of O_2 than in 2O. The three sets of curves should not be construed as showing distinct stages in the relaxation processes in the shocked gas but they do give an indication of the range of variation of T and ρ during the relaxation.

For the conditions existing in the shock-heated gas in these experiments, the argon-electron collision frequency is much less than the microwave frequency, and, the shock-heated plasma behaves like a pure dielectric. Under these conditions the electron density necessary to produce complete reflection, n_e^*, is given by[4]

$$n_e^* = \frac{\pi m_e}{e^2} f^2 \quad , \qquad (5)$$

where m_e is the electron mass, f is the microwave frequency and e is the electron charge. For $f = 1.5 \times 10^{10}$ sec^{-1}, $n_e^* = 2.8 \times 10^{12}$ electrons/cc at the lowest densities employed in this work, this corresponds to $n_e/n_{Ar} = 8 \times 10^{-5}$, which is thermally insignificant.

The microwave reflection probe was calibrated with copper

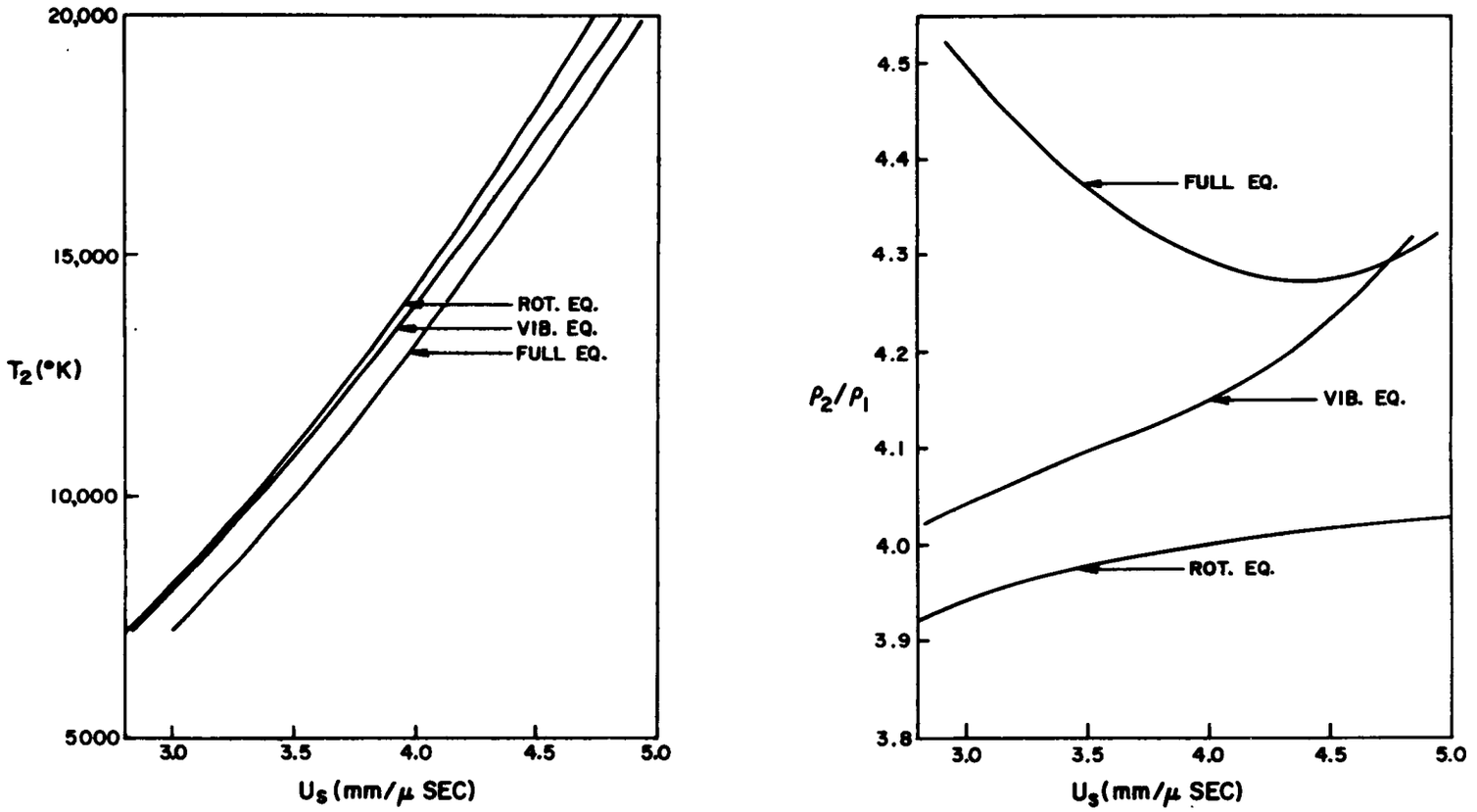

Fig. 4 Temperature (4a) and density ratio (4b) plotted vs. the shock speed for a 4% O_2 - 96% Ar mixture. All the curves are independent of initial pressure since in the pressure range of interest the oxygen dissociates completely. The three curves in each plot correspond to three different thermodynamic states of the gas. The "Full Eq." curve does not include ionization.

sheets to find its response to a perfect reflector moving across the width of the quartz window in the knife-edged plate at the end of the wave guide. In Fig. 5 the reflection coefficient, $/R/^2$, defined by the equation

$$/R/^2 = \frac{\text{power reflected}}{\text{power input}} \quad , \tag{6}$$

is plotted vs. the fraction of the quartz window covered by the copper sheet. Two different thicknesses of copper were used in this calibration, both yielding essentially the same results. Note that when the quartz window is 1/2 covered by the copper reflector, $/R/^2 = .85$.

When the microwave apparatus is mounted on the shock tube, the quartz window is bisected by the plane defined by the slits in the U. V. apparatus. Consequently, when the U. V. signal first shows the arrival of the shock wave, the microwave window is already 1/2 covered by the shocked gas. Defining t_e as the time (subsequent to the shock front arrival at the U. V. slits) when the microwave signal $/R/^2 = .85$, i. e., when $n_e \simeq n_e^*$, it is clear that if $\tau_d/t_e < 1$ no significant ionization has occurred within the chemical relaxation zone. Inspection of the dual trace oscillograms which display both the U. V. and microwave signals showed that this condition is satisfied in all cases. (For examples, see the oscillograms shown in Figs. 6, 7 and 8.)

The transmission of radiation of intensity I_0 by the shock-heated oxygen is given by the following equation:

$$I/I_0 = \exp \left[-k\ell \, (\rho_2/\rho_1) \quad (P_1/760) \, (O_2) \right] \quad , \tag{7}$$

where I/I_0 is the fraction of incident radiation transmitted, k is the absorption coefficient per cm of path length ℓ, ρ_2/ρ_1 is the density ratio across the shock front, P_1 is the initial pressure in the shock tube (mm of Hg), and (O_2) is the fraction of oxygen in the gas mixture at any time. For the mixtures studied in these experiments the temperature

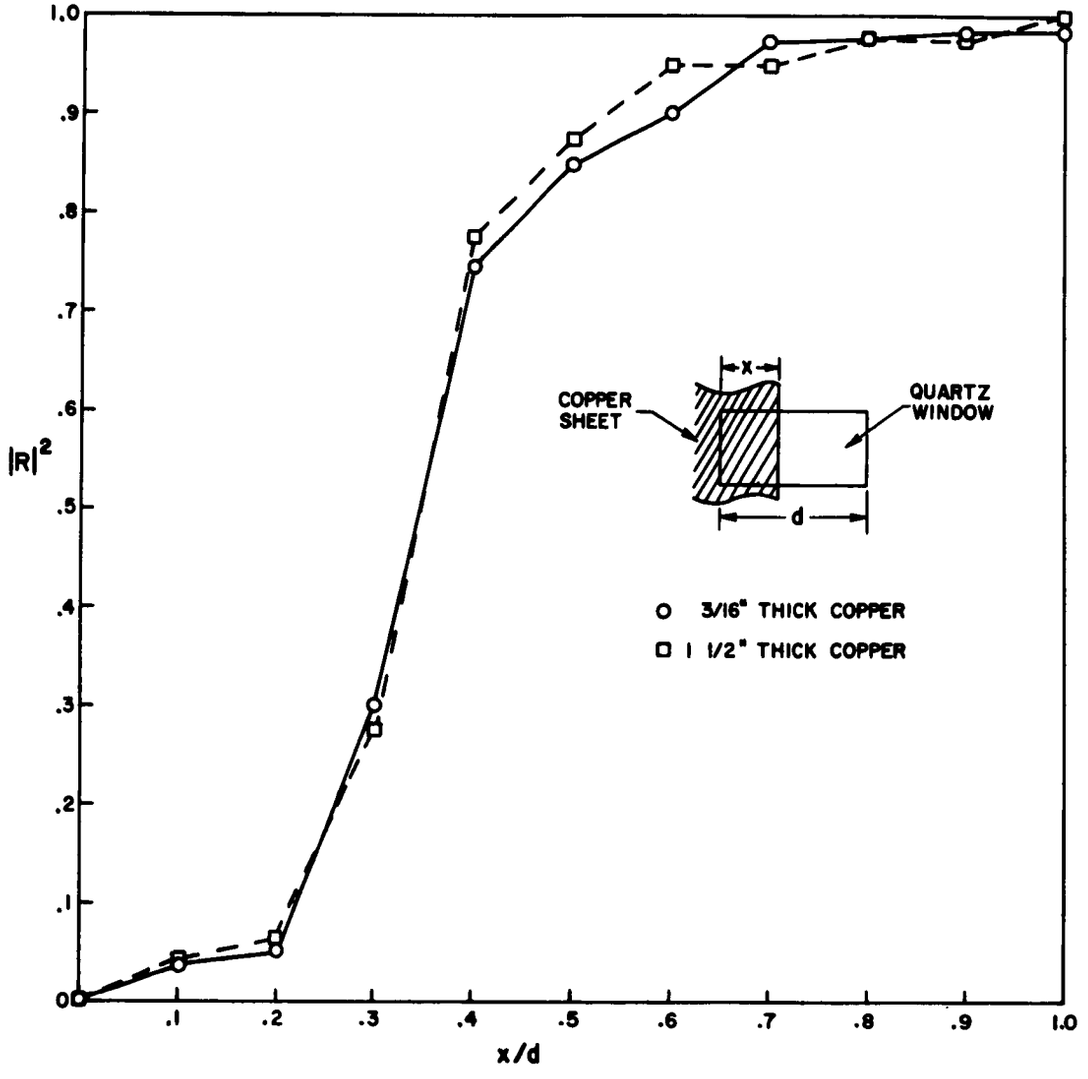

Fig. 5 Calibration of the microwave apparatus. The reflection coefficient $/R/^2$ is plotted vs. the fraction of the microwave window covered by a copper sheet.

of the shock-heated gas, T_2, and ρ_2/ρ_1 are essentially constant behind the shock. Hence, once vibrational equilibrium is obtained k is also a constant. We can therefore write

$$(O_2) = -(1/Q)\ \ln I/I_0 \quad , \tag{8}$$

where

$$Q = k \mathscr{l} (\rho_2/\rho_1)\ \ (P_1/760) = \text{constant.} \tag{9}$$

We can write the equation for the rate of disappearance of O_2 as follows

$$\frac{d \ln (O_2)}{dt_P} = \frac{d \ln (O_2)}{(\rho_2/\rho_1)dt_L} = -k_d\ (n_{Ar}/N_0) \quad , \tag{10}$$

where t_P and t_L are particle and laboratory times, respectively. Here we have neglected the contribution made by O_2 - O_2 and O_2 - O collisions due to their low frequency of occurrence (see Sec. IV for a discussion of this). Also, we have omitted the recombination term since we do not follow the process close enough to equilibrium to make this term significant.

Combination of Eqs. (8) and (10) leads to the following:

$$\frac{d \log (\log I_0/I)}{dt_L} = -\frac{k_d}{2.3}\ (n_{Ar}/N_0)\ (\rho_2/\rho_1) \quad . \tag{11}$$

A semi-log plot of $\log I_0/I$ vs. t_L should be a straight line whose slope yields k_d. Figures 6 - 9 show four such plots along with the oscillograms from which they were produced. As is seen, the data yield straight lines when plotted in this manner.

It is to be noted that the initial signal, I_i, (before shock wave

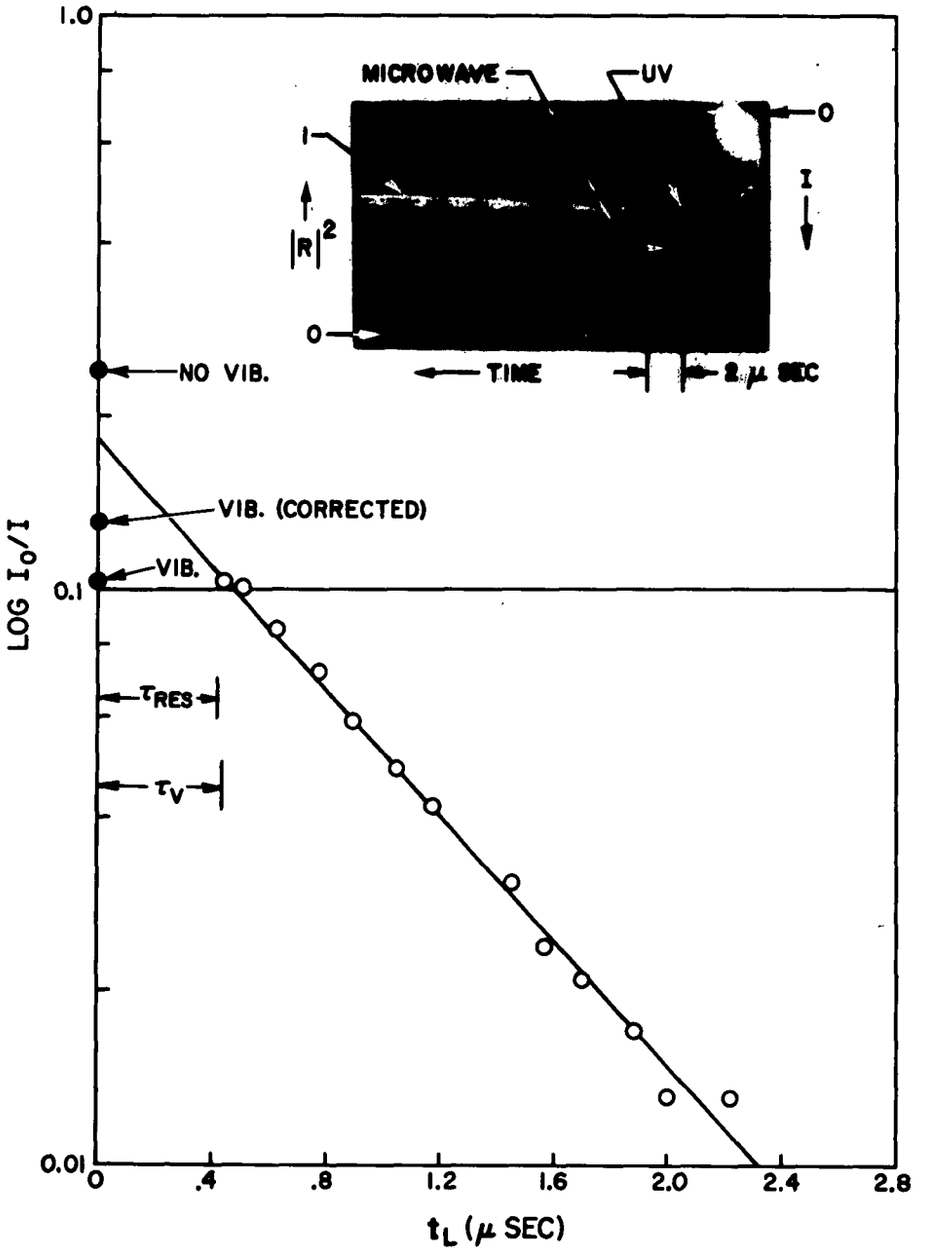

Fig. 6 Log I_0/I plotted vs. laboratory time for a particular run. The inset shows the oscillogram from which this plot was prepared. Indicated in the figure are the resolution, τ_{res}, and the vibrational relaxation time, τ_V, obtained by extrapolating the results of Ref. 2. For other notations, see text. Shock conditions: 4% O_2, P_1 = .263 mm, U_s = 4.41 mm/μsec, $\bar{T}$ = 16440°K.

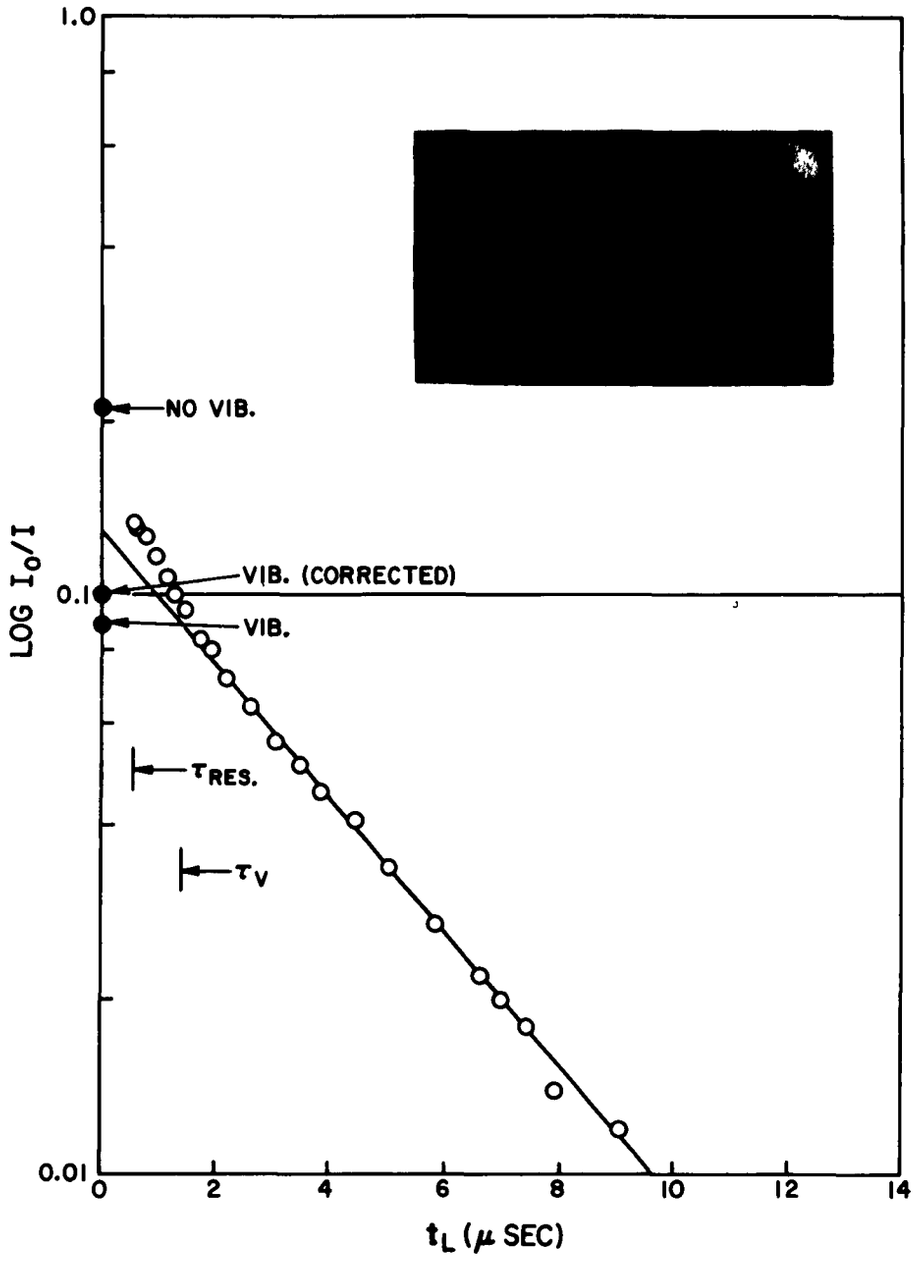

Fig. 7 Shock conditions: 4% O_2, P_1 = .236 mm, U_s = 3.53 mm/μsec, $\bar{T}$ = 10545°K.

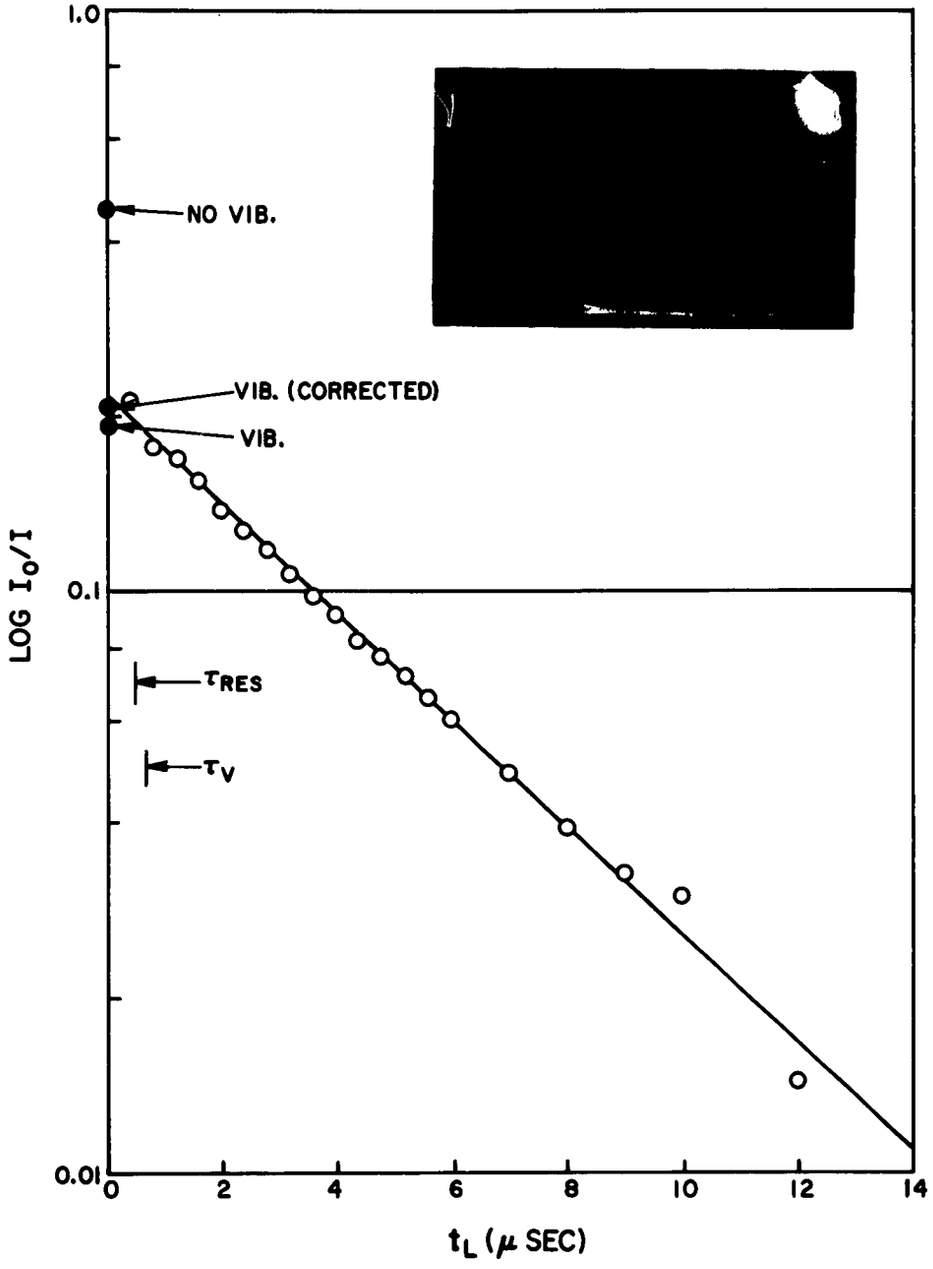

Fig. 8 Shock conditions: 2% O_2, P_1 = 1.054 mm, U_s = 3.05 mm/μsec, $\overline{T}$ = 8220°K.

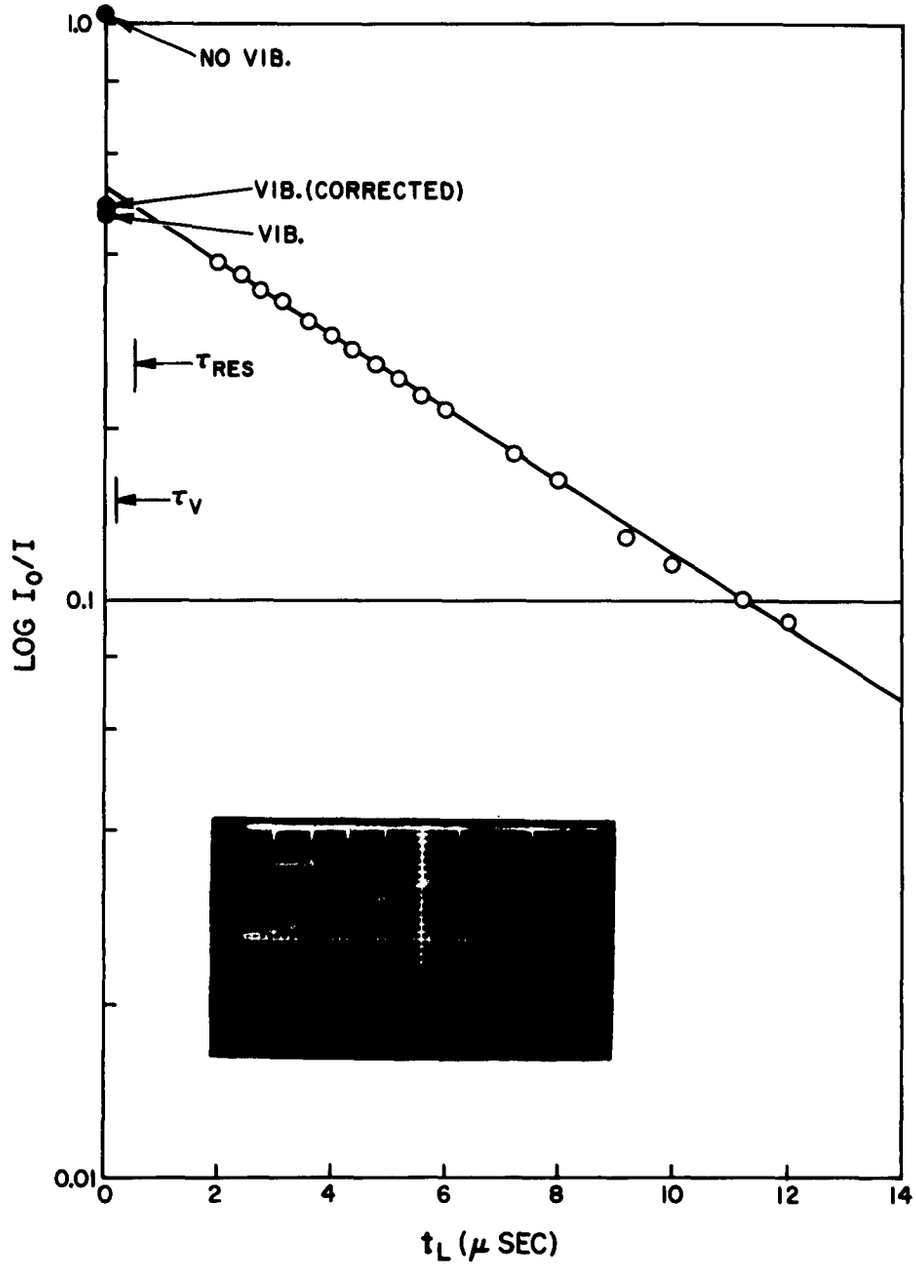

Fig. 9 Shock conditions: 1/2% O_2, P_1 = 10.09 mm, U_s = 2.56 mm/μsec, $\bar{T}$ = 6075°K.

arrival) has already been attenuated by the amount I_i/I_0. For all the runs above 7700° (4% O_2 and 2% O_2), the relaxation times were fast enough so that a measurement of I_0 could be made subsequent to dissociation. For these runs this I_0 was used in reducing the data. When the experimental value of I_i/I_0 was compared to the theoretical value calculated from Eq. (7) (setting k = 315 and $\rho_2/\rho_1 = 1$) the agreement was always within a few percent. For the low temperature runs (1/2% O_2), the relaxation times were too long to follow the signal to I_0, i.e., boundary layer build-up and change of light source intensity made this too uncertain. In these cases, the theoretical I_i/I_0 was utilized to obtain I_0.

Indicated in Figs. 6 - 9 are resolution times, τ_{res}, which were computed by the equation

$$\tau_{res} = \frac{S + \delta/4}{U_s} \quad , \tag{12}$$

where the slit width S = 1 mm, and δ is the shock front curvature given by Eq. (4). This theoretical resolution agrees well with the experimentally determined signal rise time, the exception to this being the P_1 = 4 and 10 mm runs (1/2% O_2) where, because of the high density, there was an optical effect at early times probably associated with internal reflections off the shock front.* This latter effect persisted in pure Ar shocks run at comparable densities. For this reason, these oscillograms were not read at times less than 2 μsec.

Also indicated on these figures are the vibrational relaxation times τ_v computed from Eq. (3) for the experimental conditions. The condition $\tau_v/\tau_{res} > 1$ is met in these experiments only at low densities and temperatures, in particular, for the 4% O_2 runs at the lower tempera-

* A similar effect to this was observed in previous work at 1270A, see Ref. 5.

tures at which this mixture was studied. For example, see Fig. 7 - notice how the data deviate from the straight line at $t_L < \tau_v$. Under these conditions, the absorption coefficient, k, can no longer be treated as a constant in Eq. (7), consequently, Eq. (11) is no longer valid. The upper point located on the zero time axis of Figs. 6-9 and labeled "No Vib" was calculated from Eq. (7) setting k = 315 and using the density ratio appropriate to no vibration. Notice how the data tend toward this origin in Fig. 7 for $t_L < \tau_v$.

The theoretical $t_L = 0$ intercept for these straight line plots can be computed via Eq. (7) using the value of k chosen consistent with complete vibrational equilibrium and ρ_2/ρ_1 chosen for the state "vibration only". This was done for all the runs. For Figs. 6 - 9 these points are identified as "Vib". In all except some of the lowest temperature runs (below 6500°K) the extrapolated straight line given by the data intercepts the ordinate above the theoretical point. This implies that the dissociation of O_2 does not start at zero time with the rate that is ultimately measured. Indeed, there is an incubation time, Δt, during which essentially no dissociation occurs, this time being given by the intersection of the extrapolated straight line with the "Vib" ordinate.

The zero of time was chosen from the oscillograms at the beginning of the signal. The resolution in this experiment was limited by the combination of finite slit width and shock front curvature. Because the experimental measurement of I/I_0 averaged over this finite slit and continuously looked through a gas sample which had a radial time displacement due to the shock front curvature, a slightly displaced time scale results. Using the rate constant deduced from each run, the shock conditions, the slit width and the shock front curvature, a theoretical curve was computed on an IBM 650 computer which integrated out the effect of the finite slit and shock front curvature. The pertinent equations for this procedure are derived in the Appendix. The experimental curve would be identical with this computed curve if the experimental curve actually started off with its

ultimate slope. These curves were plotted alongside the experimental curves; they were straight lines having the same slope as the experimental curve but the intercept of this computed curve fell between the intercept of the experimental curve and the theoretically computed intercept which did not take into account shock front curvature and finite slit width. The time, Δt, at which the extrapolated experimental line crossed the intercept ordinate of the computed curve represents a time during which the dissociation process is inhibited. These intercept ordinates are labeled "Vib (Corrected)" in Figs. 6 - 9.

IV. Results and Discussion

An Arrhenius plot of the dissociation rate covering the temperature range 5000 - 18000°K was constructed and is shown in Fig. 10. The temperatures, $\bar{T}$, in this figure are the average of the "Vib Eq" and the "Full Eq" temperatures. The least squares fit to the data between 5000 and 11000° yielded an O_2 - Ar dissociation rate given by the following equation

$$k_d = 2.9\ (\pm\ 12\%)\ \times 10^{14}\ \exp(-D/RT)\ \text{cc/mole-sec}, \qquad (13)$$

in which the dissociation energy of O_2 is D = 118000 cal/mole. The fit to this equation was carried out by computing the value of $k_d/\exp(-D/RT)$ for each data point and then taking the average for all the data points. The probable error was computed from the standard deviation. Although the data could have been fit with an equation having a pre-exponential temperature factor in it, as other investigators have done, it was not felt that the data warranted such treatment.

At temperatures above 11000° the data points fell below the Eq. (13) extrapolated straight line, the deviation growing larger at higher temperatures. At 18000° k_d is about 0.45 times the value given by the above equation. Also shown in Fig. 10 are the results obtained by Camac and Vaughan [Eq. (1)] which are extrapolated for T > 7500°. In a recent

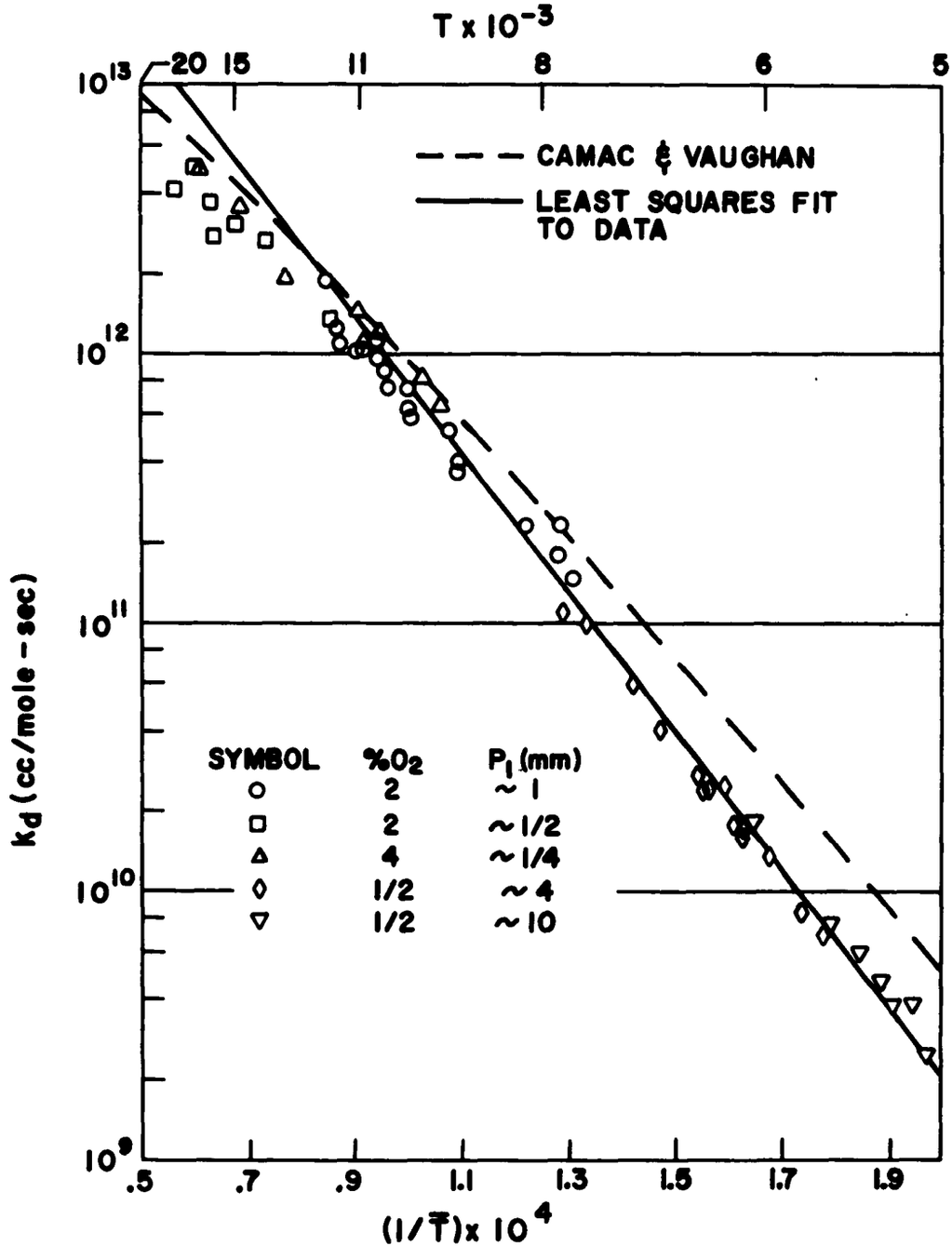

Fig. 10 The rate constant for the dissociation of O_2 by Ar plotted vs. reciprocal average temperature. The dashed line is from the work of Camac and Vaughan and is extrapolated for T > 7500°K. The least squares fit to the data shown by the solid line yields $k_d = 2.9 (\pm 12\%) \times 10^{14} \exp(-D/RT)$ cc/mole-sec.

report, Anderson,[6] in an investigation similar to that of Camac and Vaughan, gives the O_2 - Ar dissociation rate for temperatures between 4000 and 6000° as

$$k_d = 1.80 \times 10^{18} \; T^{-.98} \exp(-D/RT) \text{ cc/mole-sec.} \qquad (14)$$

This yields a rate constant 1/2 as large as that of Camac and Vaughan and therefore is in excellent agreement with the present data where the temperatures overlap (5000 - 6000°).

As was already mentioned, O_2 - O_2 and O_2 - O collisions were neglected in this work. The results of several independent investigations* indicate that, at least at low temperatures

$$k_d(O_2 - Ar) = \frac{1}{9} k_d(O_2 - O_2) = \frac{1}{25} k_d(O_2 - O) \quad . \qquad (15)$$

The low temperature work ($T < 7700°$) in this investigation was carried out with the 1/2% O_2 mixture. Concentrating our attention on the O_2 - O collision (which would, of course, have the largest effect) we find that the small increase in the effective rate constant caused by the formation of O-atoms (a factor of ≈ 1.25) is almost exactly cancelled by the decrease in the rate constant caused by the corresponding temperature drop ($\approx 115°$). On the other hand, for the 2% and 4% mixtures at high temperatures one should observe an effective rate constant which increases with time if the relations of Eq. (15) apply. For example, for the case 4% O_2 and $\bar{T} = 17000°K$, the O-atoms should increase the effective rate constant by a factor of ≈ 3 by the time the O_2 is all dissociated; the decrease in the rate constant due to the 750° temperature drop only yields an opposing factor of 0.9. Since the data yielded straight log I_0/I vs. t_L

* These are discussed and summarized in Ref. 7.

plots for the 4% O_2 cases at high temperature, it is clear that the effective rate constant is essentially constant during the dissociation process. Therefore, we conclude that in the vicinity of 17000° k_d (O_2 - O) ≈1.3 k_d (O_2 - Ar). This is not too surprising, for at 17000° the product of the collision number and the chemical relaxation time is 234, i.e., the average oxygen molecule dissociates in 234 collisions with Ar. To maintain the catalytic efficiency ratio of 25 at 17000° implies that it would take but 9 O_2 - O collisions to dissociate the average O_2. It is clear that this factor of 25 must decrease at high temperatures.

The uncorrected incubation times, all reduced to a common density (1.28×10^{17} particles/cc), are plotted vs. $T_{Vib\ Eq}$ in Fig. 11. It is to be noted that below 6500° some measured incubation times were negative and are plotted in this figure as solid symbols. One point at $T_{Vib\ Eq} = 6500$, $\Delta t_p = 0$ is not plotted.

In Fig. 12 the same data are plotted but now corrected for the effect of the finite slit width and shock front curvature as outlined in the Appendix. We have omitted the runs below 6500° for P_1 = 4 mm and below 5500° for P_1 = 10 mm because of the tremendous scatter in that data. (See discussion of errors below.) Comparison of Figs. 11 and 12 shows that the corrections to Δt (decreasing the apparent incubation time) were largest at the higher temperatures as one would expect. As seen in Fig. 12, the incubation time decreases by about two orders of magnitude between 6500 and 18000°.

In Fig. 13 we have plotted the ratio of the corrected incubation time to the vibrational relaxation time obtained from Eq. (3). The ratio $\Delta t/\tau_v$ is, of course, density independent. The solid line drawn through the data in Fig. 13 is somewhat subjective; however, it will serve to allow some comparisons to be made.

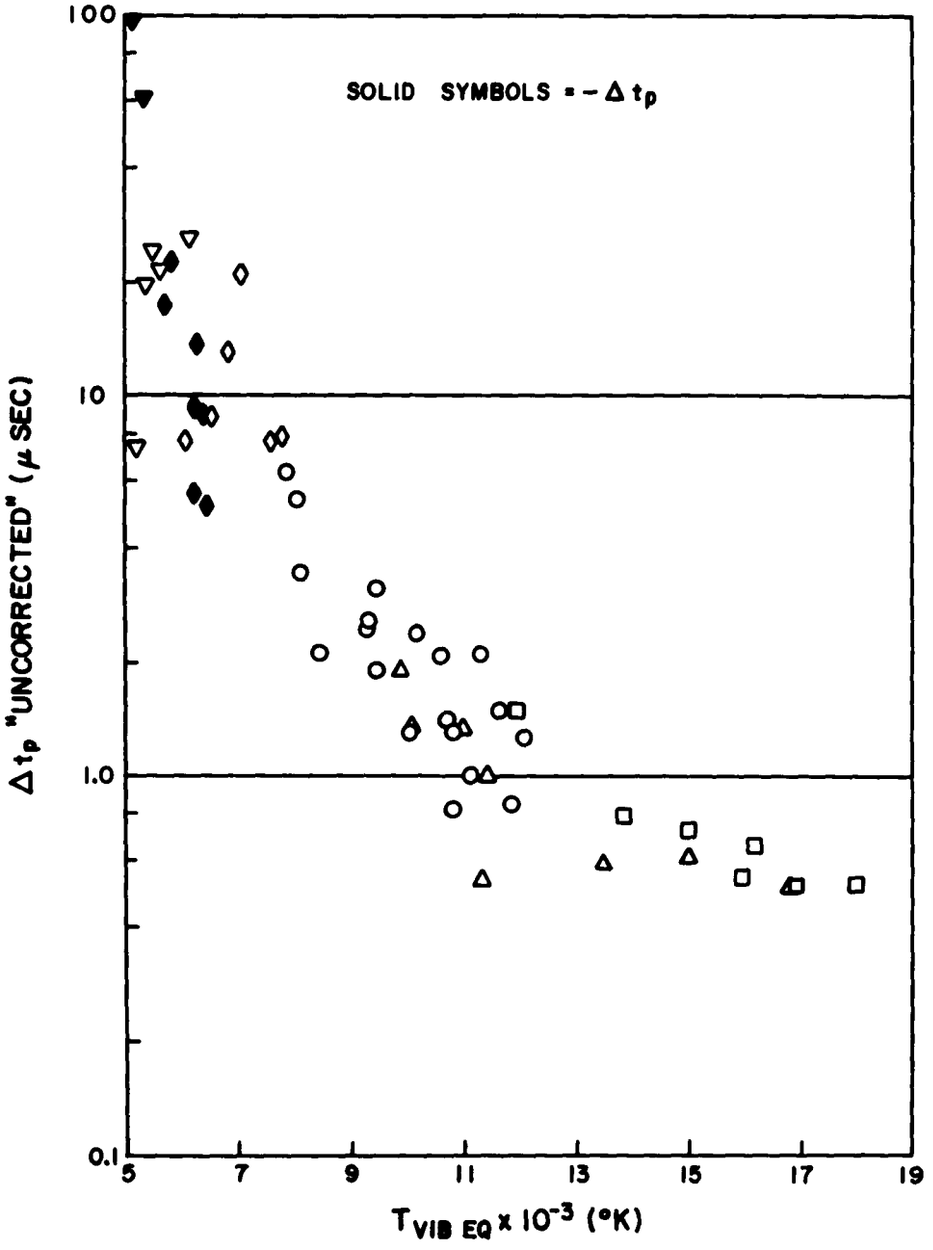

Fig. 11 The uncorrected incubation times in the particle coordinate system at a density of $n_{Ar} = 1.28 \times 10^{17}$ particles/cc plotted vs. the "Vib Eq" temperature.

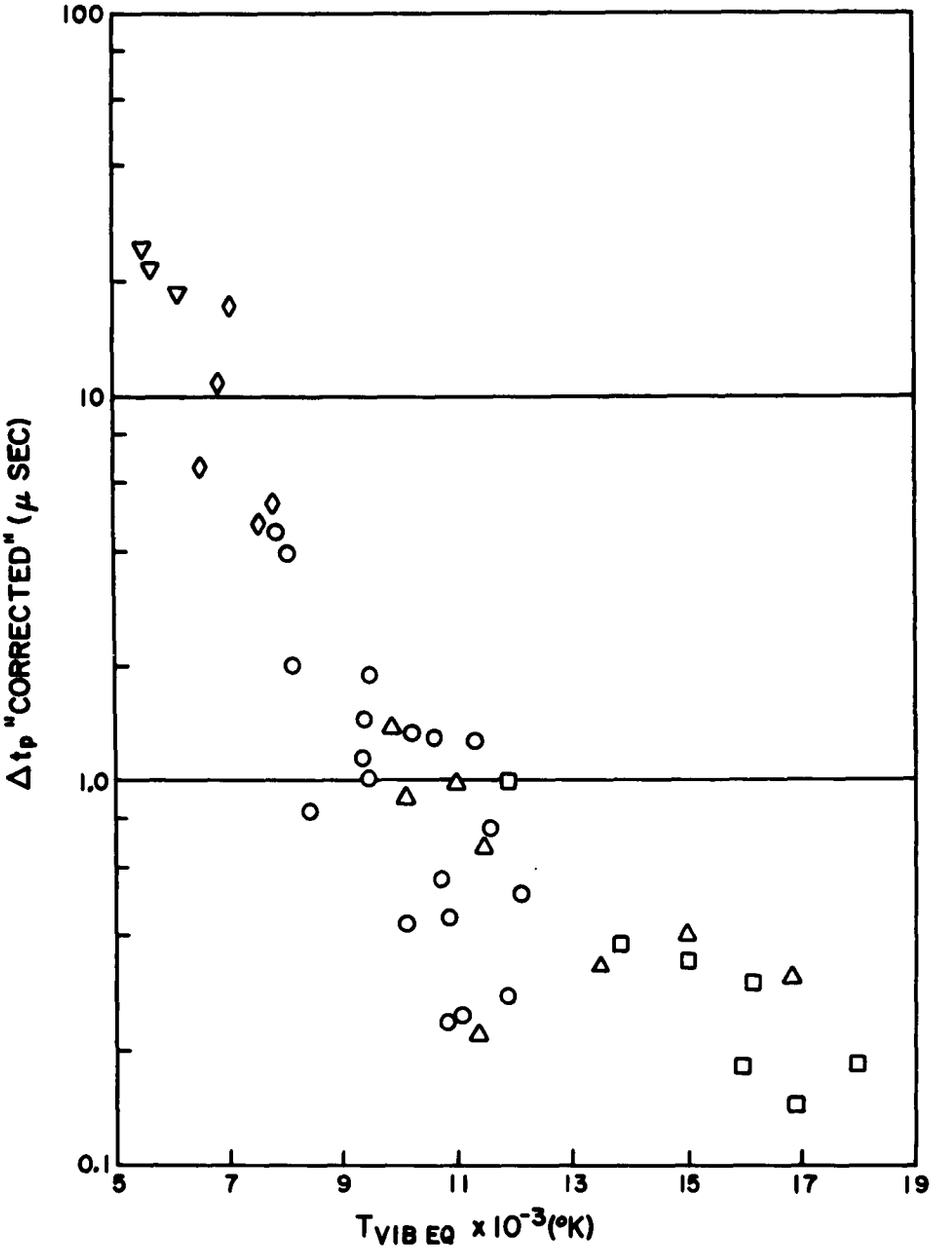

Fig. 12 The incubation times, corrected for finite slit width and shock front curvature, plotted vs. the "Vib Eq" temperature.

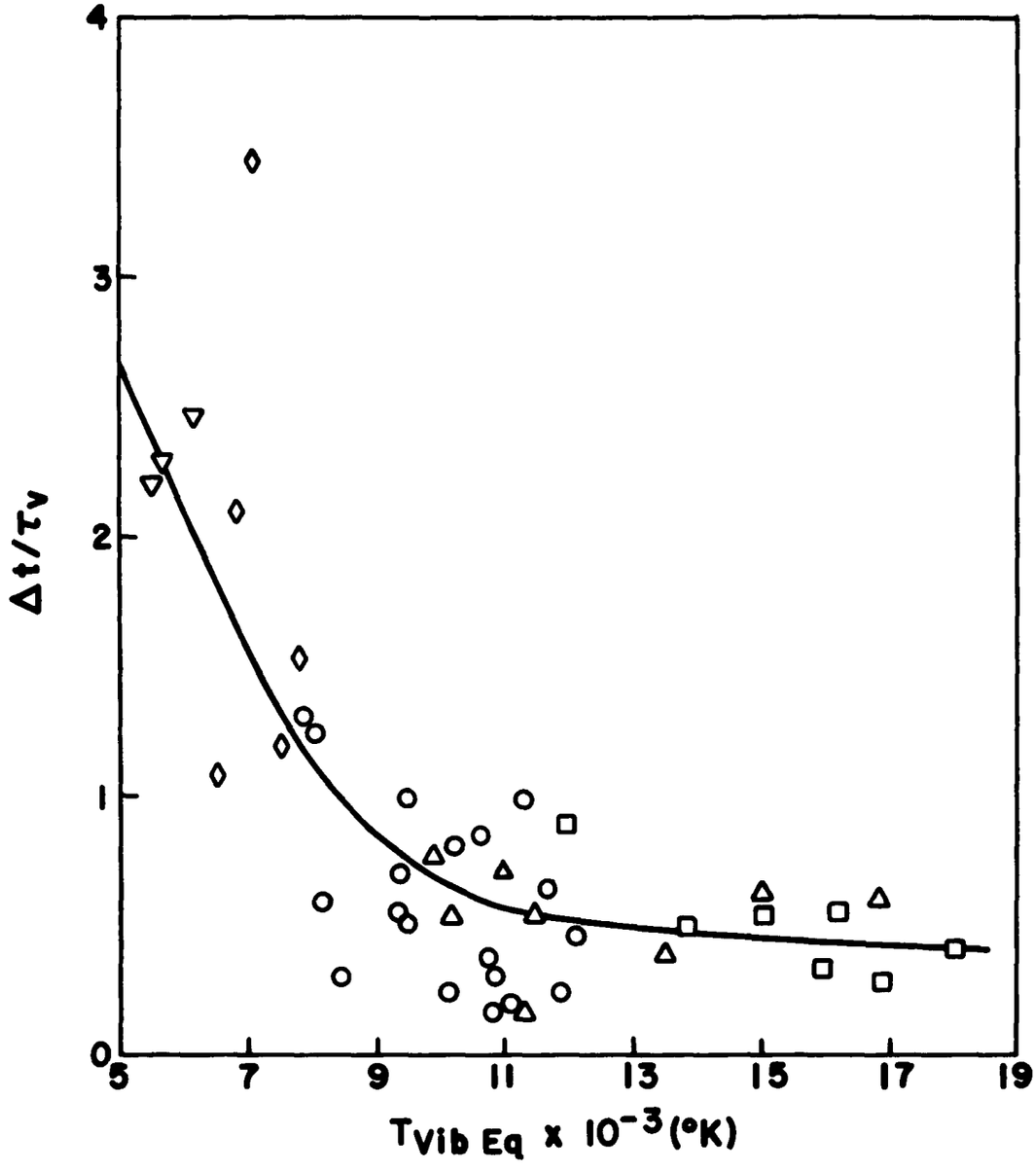

Fig. 13 The corrected incubation time divided by the vibrational relaxation time plotted vs. the "Vib Eq" temperature. The solid line drawn through the data was used in preparing Table I.

Let us define the degree of vibrational excitation, η, necessary for an uninhibited dissociation rate by the ratio

$$\eta\ (T_t) = \frac{T_v}{T_t} \quad , \tag{16}$$

where T_v and T_t are the vibrational and translational temperatures respectively. η is itself a function of translational temperature.

The vibrational energy relaxes according to the equation[8]

$$1 - \frac{E_v}{E_f} = \exp\ (-t/\tau_v) \quad , \tag{17}$$

where E_f is the vibrational energy corresponding to the final conditions and E_v is the vibrational energy at any time, t.

E_v/E_f is given by statistical mechanics as

$$\frac{E_v}{E_f} = \frac{\exp\ (\theta/T_f) - 1}{\exp\ (\theta/T_v) - 1} \quad , \tag{18}$$

where T_f is the final vibrational temperature consistent with E_f and T_v is the vibrational temperature corresponding to E_v. For O_2, $\theta = 2228^{\circ}K$.

We wish to calculate $T_v/T_t = \eta$ when the time $t = \Delta t$. Noting that the final vibrational temperature, T_f, is identical with the translational temperature T_t, we combine Eqs. (16), (17) and (18) to give

$$\frac{\Delta t}{\tau_v} = \ln \left\{ \frac{\exp\ (\theta/\eta\, T_t) - 1}{\exp\ (\theta/\eta\, T_t) - \exp\ (\theta/T_t)} \right\} \quad . \tag{19}$$

In Table I we give η calculated from Eq. (19) at several temperatures. The $\Delta t/\tau_v$ at each temperature corresponds to the solid line in Fig. 13.

Table I

T_t	$\Delta t/\tau_v$	$\eta = T_v/T_t$
5500	2.4	.93
8000	1.1	.71
11000	.55	.48
14000	.45	.41
18000	.40	.37

Although the scatter in the data is considerable, the results clearly indicate that the dissociation rate of O_2 is severely limited until some degree of vibrational equilibration obtains, the degree of equilibration necessary being higher at lower translational temperatures.

The largest source of error in this work is due to the uncertainty in I_0. This is caused by a combination of reading errors on the oscillograms, boundary layer effects, and light intensity variation.

The straight line of Eq. (11) can be represented by

$$y \equiv \log (\log I_0/I) = a\, t + b \quad . \tag{20}$$

Eq. (20) yields

$$\Delta t = (y_0 - b)/a \quad , \tag{21}$$

where y_0 is the ordinate at $t = \Delta t$. For the two coordinates (y_2, t_2) and (y_1, t_1) we have

$$a = \frac{y_2 - y_1}{t_2 - t_1} \quad \text{and} \quad b = \frac{y_1\, t_2 - y_2\, t_1}{t_2 - t_1} \quad . \tag{22}$$

Differentiation of the above equations yields the following relations:

$$\Delta y = (.189)\ 10^{-y}\ \frac{\Delta I_0}{I_0} \tag{23}$$

$$\frac{\Delta a}{a} = \frac{\Delta y_2 - \Delta y_1}{y_2 - y_1}$$

$$\frac{\Delta b}{a} = \frac{\Delta y_1 \, t_2 - \Delta y_2 \, t_1}{y_2 - y_1} \qquad (23) \text{ (Cont.)}$$

$$\frac{\Delta (\Delta t)}{\Delta t} = -\frac{\Delta b}{a \, \Delta t} - \frac{\Delta a}{a} \quad .$$

With the aid of these equations, the fractional errors $\Delta(\Delta t)/\Delta t$ and $\Delta a/a$ were computed at several temperatures using typical values of Δt, y_1, y_2, t_1 and t_2 consistent with the experiment. These errors are tabulated in Table II. We have taken $\Delta I_0/I_0$ to be $\pm$ 4.0×10^{-2}, which is probably an upper limit to the uncertainty in $\Delta I_0/I_0$.

Table II

$\Delta I_0/I_0$ assumed $\pm$ 0.04

$T^\circ K$	P_1(mm)	$\Delta(\Delta t)/\Delta t$	$\Delta a/a$
5500	10	$\pm$ 1.3	$\mp$ .052
6000	10	$\pm$ .58	$\mp$ .094
6000	4	$\pm$ 2.2	$\mp$ .14
8000	1	$\pm$ 1.0	$\mp$ .55
12000	1/2	$\pm$ .53	$\mp$ .68
17000	1/4	$\pm$ .14	$\mp$ .68

These error calculations are the bases for discarding the Δt data below 6500° for the 4 mm runs and below 5500° for the 10 mm runs. Notice that these error calculations indicate a larger fractional error in the rate constant ($\Delta a/a$) at the higher temperatures. Inspection of Fig. 10 bears this out.

V. Acknowledgment

The author wishes to acknowledge the aid given him by Dr. M. Litvak in the work presented in the Appendix. He also wishes to thank Mr. A. Magro and Mr. W. Fyfe for their help in carrying out the experimental program.

APPENDIX

Here we derive the equation analogous to Eq. (11) but embodying corrections for the shock front curvature and finite slit width. The following sketch will be necessary to define the problem.

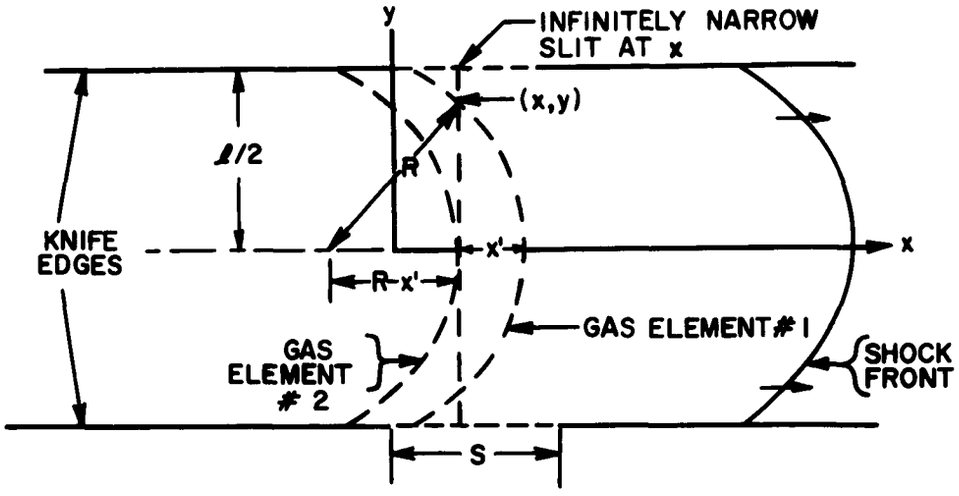

The shock front (curvature exaggerated in this sketch) has moved across the finite slits of width S (exaggerated width) from left to right. Time equals zero when the shock arrived at the position $x = y = 0$. Two gas elements are shown by the dashed curves. It is clear that

$$(R - x')^2 + y^2 = R^2 \quad , \qquad \text{(A-1)}$$

and, ignoring the small $(x')^2$ term,

$$x' = y^2/2R \quad ; \qquad \delta = (\ell/2)^2/2R \quad , \qquad \text{(A-2)}$$

where the δ is understood to be the shock front curvature existing between the knife edges.

We define the time t' to be the time elapsed between the arrival of the shock front (along y = 0) at the infinitely narrow slit and the arrival of the gas element #2; i.e.,

$$t' = t - x/U_s \qquad . \qquad (A\text{-}3)$$

It is clear, however, that the time the gas has been heated decreases as we move out from y = 0 to y = $\ell/2$; indeed, at the point (x, y) we are looking at gas (in gas element #1) which has been heated for a time given by

$$t'' = t' - x'/U_s \qquad . \qquad (A\text{-}4)$$

This is perfectly general and t'' is the time which appears in the exponential decay law for the O_2 dissociation. We can now write

$$(O_2) = \exp\left[-(t' - x'/U_s)/\tau\right] = \left[\exp(-t'/\tau)\right]\left[\exp(y^2/2R\,U_s\tau)\right], \qquad (A\text{-}5)$$

where τ is the dissociation relaxation time defined by Eq. (2) but in the laboratory coordinate system.

The absorption equation [Eq. (7)] written in differential form is

$$d \ln I/I_0 = - Q\,(O_2)\,dy \qquad , \qquad (A\text{-}6)$$

where Q is defined in Eq. (9). Elimination of (O_2) between (A-5) and (A-6) and integration across the optical path from $-\ell/2$ to $+\ell/2$ yield

$$\frac{I}{I_0} = \exp\left\{-2\,Q\exp(-t'/\tau)\int_0^{\ell/2}\exp(y^2/2\,R\,U_s\,\tau)\,dy\right\} \qquad . \qquad (A\text{-}7)$$

Making the substitution

$$y' = y/(2R\ U_s\ \tau)^{1/2} \quad , \qquad \text{(A-8)}$$

and with the aid of (A-2), we find (A-7) becomes

$$I/I_0 = \exp\left[-Q\ \ell\ \beta\ \exp(-t'/\tau)\right] \quad , \qquad \text{(A-9)}$$

where

$$\beta = \left(\frac{U_s\tau}{\delta}\right)^{1/2} \int_0^{\left(\frac{\delta}{U_s\tau}\right)^{1/2}} \exp(y')^2\, dy' \qquad \text{(A-10)}$$

The next step is to average over the finite slit, hence we write

$$\int_0^S \frac{I}{I_0}\ \frac{dx}{S} = \int_0^S \exp\left[-Q\ell\beta\ \exp(-t'/\tau)\right] \frac{dx}{S} \quad , \qquad \text{(A-11)}$$

and making the substitution

$$Z = x/U_s\tau \quad , \qquad \text{(A-12)}$$

we have

$$\frac{I}{I_0} = \left(\frac{U_s\tau}{S}\right) \int_0^{\frac{S}{U_s\tau}} \exp\left[-Q\ell\ \beta\ \exp(-t/\tau)\ \exp(Z)\right] dZ. \qquad \text{(A-13)}$$

Defining

$$\gamma \equiv Q\ell\ \beta\ \exp(-t/\tau) \quad , \qquad \text{(A-14)}$$

which is independent of x, and making the substitution

$$U = \gamma \exp Z \quad , \tag{A-15}$$

we find

$$\frac{I}{I_0} = \left(\frac{U_s \tau}{S}\right) \int_{\gamma}^{\gamma} \exp\,(S/U_s \tau)\ \exp\,(-U)\ \frac{dU}{U} \quad . \tag{A-16}$$

For a given shock tube run, $\delta/U_s \tau$ is known; hence β can be evaluated from (A-10) and is independent of time, and γ can be evaluated from (A-14) as a function of time and the corrected I/I_0 can be calculated from (A-16) as a function of time.

REFERENCES

1. M. Camac and A. Vaughan, J. Chem. Phys. 34, 460 (1961).
2. M. Camac, J. Chem. Phys. 34, 448 (1961).
3. S. C. Lin and W. Fyfe, Phys. of Fluids 4, 238 (1961).
4. S. C. Lin, R. Neal and W. Fyfe, "Rate of Ionization Behind Shock Waves in Air 1. Experimental Results", Avco-Everett Research Laboratory, Research Report 105, September 1960.
5. K. L. Wray and J. D. Teare, "A Shock Tube Study of the Kinetics of Nitric Oxide at High Temperatures", Avco-Everett Research Laboratory, Research Report 95, June 1961.
6. O. L. Anderson, "Shock Tube Measurements of Oxygen Dissociation Rates in Argon", United Aircraft Corporation, Research Laboratories, Report R-1828-1, August 1961.
7. K. L. Wray, "The Chemical Kinetics of High Temperature Air", Avco-Everett Research Laboratory, Research Report 104, June 1961.
8. E. Montroll and K. Shuler, J. Chem. Phys. 26, 454 (1957).

Avco-Everett Research Laboratory, Everett, Massachusetts
A SHOCK TUBE STUDY OF THE COUPLING OF THE O_2-Ar RATES OF DISSOCIATION AND VIBRATIONAL RELAXATION, by Kurt L. Wray. January 1962, 35 p. incl. illus. (Avco-Everett Research Report 125)
(Contract DA-19-020-ORD-5476)

Unclassified report

At low temperatures the vibrational relaxation time, r_v, is much shorter than the dissociation time, r_d. The O_2-Ar results of Camac (J. Chem. Phys. 34, 448 (1961)) and Camac and Vaughan (Ibid, p. 460) yield a $r_d/r_v = 60$ at 5000°K and, upon extrapolation, a $r_d/r_v = 1.4$ at 18000°. According to these extrapolations, dissociation at high temperatures would proceed significantly before vibrational equilibration would occur. The purpose of this investigation was to determine how the dissociation rate will be affected by a lack of vibrational equilibrium. Studies of the dissociation rate of dilute O_2 - Ar mixtures were made in a 24" diameter shock tube from 5000-18000°K. The O_2 concentration was monitored by its absorption of 1470A radiation. An Arrhenius plot of the data yielded

(over)

UNCLASSIFIED

1. Oxygen-Argon mixtures-Dissociation.
2. Oxygen-Argon mixtures-Vibrational relaxation.
3. Oxygen-Argon mixtures-Shock tube studies.
4. Shock tubes-Application.

I. Title.
II. Wray, Kurt L.
III. Avco-Everett Research Report 125.
IV. Contract DA-19-020-ORD-5476

UNCLASSIFIED

Avco-Everett Research Laboratory, Everett, Massachusetts
A SHOCK TUBE STUDY OF THE COUPLING OF THE O_2-Ar RATES OF DISSOCIATION AND VIBRATIONAL RELAXATION, by Kurt L. Wray. January 1962, 35 p. incl. illus. (Avco-Everett Research Report 125)
(Contract DA-19-020-ORD-5476)

Unclassified report

At low temperatures the vibrational relaxation time, r_v, is much shorter than the dissociation time, r_d. The O_2-Ar results of Camac (J. Chem. Phys. 34, 448 (1961)) and Camac and Vaughan (Ibid, p. 460) yield a $r_d/r_v = 60$ at 5000°K and, upon extrapolation, a $r_d/r_v = 1.4$ at 18000°. According to these extrapolations, dissociation at high temperatures would proceed significantly before vibrational equilibration would occur. The purpose of this investigation was to determine how the dissociation rate will be affected by a lack of vibrational equilibrium. Studies of the dissociation rate of dilute O_2 - Ar mixtures were made in a 24" diameter shock tube from 5000-18000°K. The O_2 concentration was monitored by its absorption of 1470A radiation. An Arrhenius plot of the data yielded

(over)

UNCLASSIFIED

1. Oxygen-Argon mixtures-Dissociation.
2. Oxygen-Argon mixtures-Vibrational relaxation.
3. Oxygen-Argon mixtures-Shock tube studies.
4. Shock tubes-Application.

I. Title.
II. Wray, Kurt L.
III. Avco-Everett Research Report 125.
IV. Contract DA-19-020-ORD-5476.

UNCLASSIFIED

a straight line from 5000-11000°K, the rate constant being given by $k_d = 2.9 (\pm 12\%) \times 10^{14} \exp(-D/RT)$ cc/mole-sec. Above 11000° the data deviate from the line given by this equation - at 18000°K k_d being .45 times the calculated value. An incubation time, Δt, was observed during which dissociation does not proceed to a significant extent. The ratio of this incubation time to the vibrational relaxation time (obtained by extrapolating Camac's low temperature results) when plotted against translational temperature, displays a slight negative temperature dependence. At 18000° $\Delta t/r_v = 0.4$, at 8000° $\Delta t/r_v = 1$, and at 5500° we estimate that $\Delta t/r_v \approx 2$.

UNCLASSIFIED

a straight line from 5000-11000°K, the rate constant being given by $k_d = 2.9 (\pm 12\%) \times 10^{14} \exp(-D/RT)$ cc/mole-sec. Above 11000° the data deviate from the line given by this equation - at 18000°K k_d being .45 times the calculated value. An incubation time, Δt, was observed during which dissociation does not proceed to a significant extent. The ratio of this incubation time to the vibrational relaxation time (obtained by extrapolating Camac's low temperature results) when plotted against translational temperature, displays a slight negative temperature dependence. At 18000° $\Delta t/r_v = 0.4$, at 8000° $\Delta t/r_v = 1$, and at 5500° we estimate that $\Delta t/r_v \approx 2$.

UNCLASSIFIED